α- and β-Deuterium Isotope Effects in the MgX_2 and Methylaluminoxane Promoted Intramolecular Olefin Insertion of Cp_2TiClR Complexes. Insight into Cocatalyst Dependence and Chain End Control in Ziegler–Natta Polymerization

Nancy S. Barta,† Brian A. Kirk, and John R. Stille*,‡

Contribution from the Department of Chemistry, Michigan State University, East Lansing, Michigan 48824-1322

Received November 4, 1993. Revised Manuscript Received March 14, 1994®

Abstract: Participation of α- and β-hydrogens in the intramolecular insertion of an α-olefin into a titanium–carbon bond was examined through competitive cyclization of isotopically labeled 2-alkyl-6-hepten-1-yl ligands. Comparison of cyclization rates revealed deuterium isotope effects for both the α and β sites of a propagating chain model (L_nMCH_2-$CHRCH_2P$) in which the α-, β-, and γ-positions of the ligand reflected the structural features of a propagating poly α-olefin chain. In particular, the polymerizations of 1-pentene (R = *n*-propyl) and 1-hexene (R = *n*-butyl) were modeled. Through the use of MgX_2 to promote alkene insertion, unusual mechanistic features of this insertion process were observed in which both α- and β-agostic interactions were involved in the rate determining step of olefin insertion. The k_H/k_D values for the α-position were 1.22 ± 0.03 and 1.28 ± 0.03 for the *n*-propyl and *n*-butyl substrates, respectively, while the k_H/k_D values for the β-position were 1.09 ± 0.02 and 1.10 ± 0.02 for these substrates. When both sites were labeled, α- and β-hydrogens worked in concert to produce a k_H/k_D of 1.36 ± 0.03. In contrast, when insertion was promoted by methylaluminoxane, an inverse deuterium isotope effect was observed for the α-hydrogen, with a k_H/k_D for the α-hydrogen participation of 0.88 ± 0.04 and 0.95 ± 0.04 for the *n*-propyl and *n*-butyl substrates, respectively. An opposite but complementary effect was observed for β-hydrogen participation, for which a k_H/k_D value of 1.06 ± 0.04 was obtained for each substrate.

Introduction

Ziegler–Natta polymerization of α-olefins, a process which forms hundreds of carbon–carbon bonds sequentially with high stereoselectivity, is one of the most efficient and intriguing organic reactions known.[1] However, despite the intense interest in this reaction, the mechanistic details of this process have remained elusive for almost 40 years. The heterogeneous nature of the most effective catalyst mixtures has made these processes inherently difficult to study, and the majority of mechanistic information for these systems has been acquired through work with homogeneous catalysts.

The introduction of methylaluminoxane (MAO) as a cocatalyst for Ziegler–Natta polymer formation produced a revolutionary advancement in the science of homogeneous α-olefin polymerization.[2] With the use of this unique cocatalyst mixture, either isotactic or syndiotactic polymer formation could be obtained through ligand-directed enantiomorphic site control. However, for catalyst systems such as Cp_2TiPh_2/MAO, which lack sterically dominating metallocene ligands, the selective formation of isotactic polypropylene resulted from the subtle effects of 1,3-asymmetric induction from the polymer stereocenter β to the titanium (chain end control).[2] In contrast, related Cp_2ZrMe_2/MAO catalyst systems[3] produced atactic polypropylene.[4] The same pattern has been observed in the formation of polystyrene, in which Cp_2TiCl_2/MAO stereoselectively produced syndiotactic polymer, while the product generated by Cp_2ZrCl_2/MAO was atactic.[5] The origin of the differences between these related titanium and zirconium catalyst systems remains undefined.

As a way to rationalize stereoselective polymer formation in Ziegler–Natta systems, participation of the growing polymer chain was invoked as a key feature of the olefin insertion reaction. Initially, Green and Rooney suggested the possibility of an α-hydrogen migration,[6] and this proposal was latter modified to involve intermediate α-hydrogen agostic interactions.[7] Since that time, agostic participation of hydrogens in both ground state stabilization and olefin insertion has been studied extensively through theoretical calculations.[8] In an effort to acquire

† Division of Organic Chemistry of the American Chemical Society Graduate Fellowship recipient, sponsored by Pfizer, Inc., 1993–1994.

‡ Present address: Chemical Process Research and Development, Lilly Research Laboratories, Indianapolis, IN 46285-4813.

® Abstract published in *Advance ACS Abstracts,* August 15, 1994.

(1) For recent reviews in Ziegler–Natta polymeriation, see: (a) Kissin, Y. V. *Isospecific Polymerization of Olefins with Heterogeneous Ziegler–Natta Catalysts*; Springer-Verlag: New York, 1985. (b) Minsker, K. S.; Karpasas, M. M.; Zaikov, G. E. *Russ. Chem. Rev.* **1986**, *55*, 17. (c) Tait, P. J. T., Allen, G., Bevington, J. C., Eds. *Comprehensive Polymer Science*; Pergamon Press: Oxford, 1989; Chapter 1. (d) Tait, P. J. T., Watkins, N. D., Allen, G., Eds. *Comprehensive Polymer Science*; Pergamon Press: Oxford, 1989; Chapter 2. (e) Krenstel', B. A.; Nekhaeva, L. A. *Russ. Chem. Rev.* **1990**, *59*, 1193. (f) Skupinska, J. *Chem. Rev.* **1991**, *91*, 613. (g) Odian, G. *Principles of Polymerization*; Wiley: New York, 1991; Chapter 8.

(2) (a) Ewen, J. A. *J. Am. Chem. Soc.* **1984**, *106*, 6355. (b) Ewen, J. A. *Catalytic Polymerization of Olefins*; Keii, T., Soga, K., Eds.; Elsevier: New York, 1986; p 271. (c) Zambelli, A.; Ammendola, P.; Grassi, A.; Longo, P.; Proto, A. *Macromolecules* **1986**, *19*, 2703. (d) Zambelli, A.; Longo, P.; Ammendola, P.; Grassi, A. *Gazz. Chim. Ital.* **1986**, *116*, 731.

(3) (a) Sinn, H.; Kaminsky, W.; Vollmer, H.-J.; Woldt, R. *Angew. Chem., Int. Ed. Engl.* **1980**, *19*, 390. (b) Sinn, H.; Kaminsky, W. *Adv. Organomet. Chem.* **1980**, *18*, 99.

(4) For an example of chain end control by a zirconium catalyst, see: Erker, G.; Nolte, R.; Tsay, Y.-H.; Krüger, C. *Angew. Chem., Int. Ed. Engl.* **1989**, *28*, 628.

(5) Ishihara, N.; Kuramoto, M.; Uoi, M. *Macromolecules* **1988**, *21*, 3356.

(6) (a) Ivin, K. J.; Rooney, J. J.; Stewart, C. D.; Green, M. L. H.; Mahtab, R. *J. Chem. Soc., Chem. Commun.* **1978**, *604*. (b) Green, M. L. H. *Pure Appl. Chem.* **1978**, *50*, 27.

(7) (a) Dawoodi, Z.; Green, M. L. H.; Mtetwa, V. S. B.; Prout, K. *J. Chem. Soc., Chem. Commun.* **1982**, 1410. (b) Brookhart, M.; Green, M. H. L. *J. Organomet. Chem.* **1983**, *250*, 395. (c) Brookhart, M.; Green, M. H. L.; Wong, L.-L. *Prog. Inorg. Chem.* **1988**, *36*, 1.

(8) For theoretical treatment of agostic interactions in Ziegler–Natta olefin insertions, see: (a) Prosenc, M.-H.; Janiak, C.; Brintzinger, H.-H. *Organometallics* **1992**, *11*, 4036. (b) Kawamura-Kuribayashi, H.; Koga, N.; Morokuma, K. *J. Am. Chem. Soc.* **1992**, *114*, 2359. (c) Kawamura-Kuribayashi, H.; Koga, N.; Morokuma, K. *J. Am. Chem. Soc.* **1992**, *114*, 8687. (d) Gleiter, R.; Hyla-Krypsin, I.; Niu, S.; Erker, G. *Organometallics* **1993**, *12*, 3828. (e) Janiak, C. *J. Organomet. Chem.* **1993**, *452*, 63 and references therein.

0002-7863/94/1516-8912$04.50/0

experimental evidence for α-hydrogen agostic interactions during olefin insertions, elegant deuterium isotope effect studies were used to probe stereoselective product formation through internally competitive interaction of an α-hydrogen and α-deuterium with the active metal center. This approach was first used to model the ethylene polymerization catalyst $Cp_2TiEtCl/EtAlCl_2$, but α-hydrogen participation was not observed in the formation of **2** from **1** (eq 1).[9] Similarly, intramolecular five-membered ring formation with a zirconocene/MAO system did not produce measurable effects for α-hydrogen participation.[10]

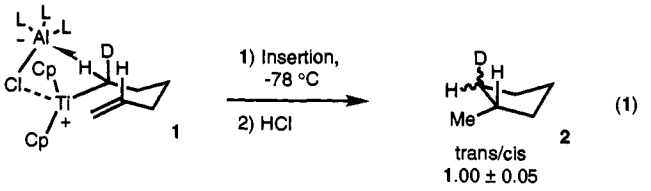

(1)

With the use of a less conformationally restricted intermolecular approach, a 1.30:1.00 (±0.03) ratio of *erythro*-**5**/*threo*-**5** was observed for α-olefin insertion into **3** (Scheme 1).[10] These results demonstrated a preference for transition state (α-H)-**4** over that of (α-D)-**4** and confirmed the participation of α-hydrogens in the rate-determining step of stereoselective chain propagation.[8,10,11] In the absence of a Lewis acid cocatalyst, a scandium catalyst produced stereoselective cyclopentane formation (1.19:1.00 (±0.04)) with the intramolecular cyclization strategy used for transformation of **1** to **2**.[12] In each of these examples, the complexes that were examined had the general structure $L_nMCHDCH_2CH_2P$, in which the α-, β-, and γ-positions of the catalyst ligand modeled the repeating methylene units of a propagating polyethylene chain.

Scheme 1. Evidence for α-H Activation in a Methylaluminoxane (MAO) Activated System

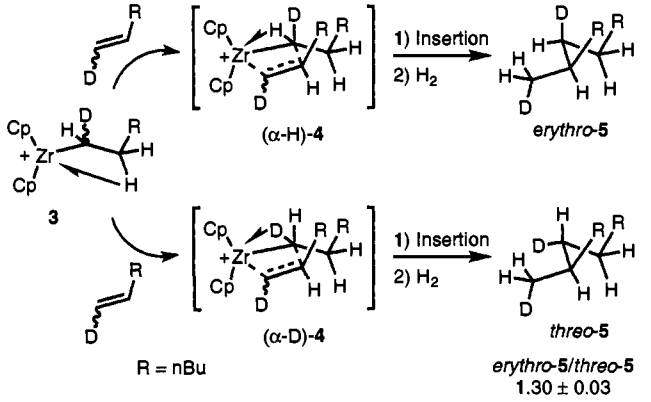

Earlier investigations from these laboratories, which explored intramolecular insertion as a model for polymerization, revealed a dependence of the stereoselective cyclization of **6** to **7** on the Lewis acid additive and reaction temperature (eq 2).[13] In an effort to expand the understanding of this and related cyclization systems,[14] we initiated an investigation to probe the role of the Lewis acid. These systems possess the structural features of a propagating poly α-olefin chain at the α-, β-, and γ-positions and can be used to gain insight into the dependence of chain end control upon the Lewis acid cocatalyst in titanium-based Ziegler–Natta polymerization systems.

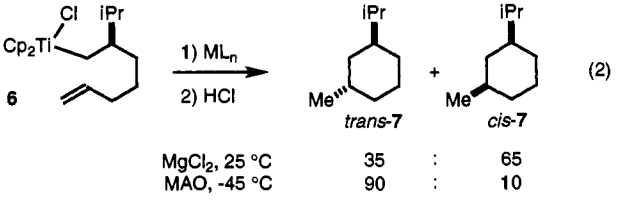

(2)

Results and Discussion

System Design. Examination of kinetic isotope effects in cyclization systems which model α-olefin polymerization ($L_nMCH_2CHRCH_2P$, R = alkyl) presented unique challenges. The effect of a β-alkyl substituent on chain participation in the insertion process could not be established through internally competitive α- and β-hydrogen interactions since the α-hydrogens are diastereotopic and only a single β-hydrogen is present. Instead, an alternative approach was designed in which deuterium isotope effects were examined through competitive intramolecular six-membered ring formation of selectively deuterated substrates related in structure to **6** (eq 2).[15] Labeled substrates were differentiated with the use of *n*-propyl (**a**) and *n*-butyl (**b**) substituents at the β-position, which represented the propagating polymer chains of 1-pentene and 1-hexene, respectively (Scheme 2).[16]

Scheme 2. Synthesis of Cyclization Substrates[a]

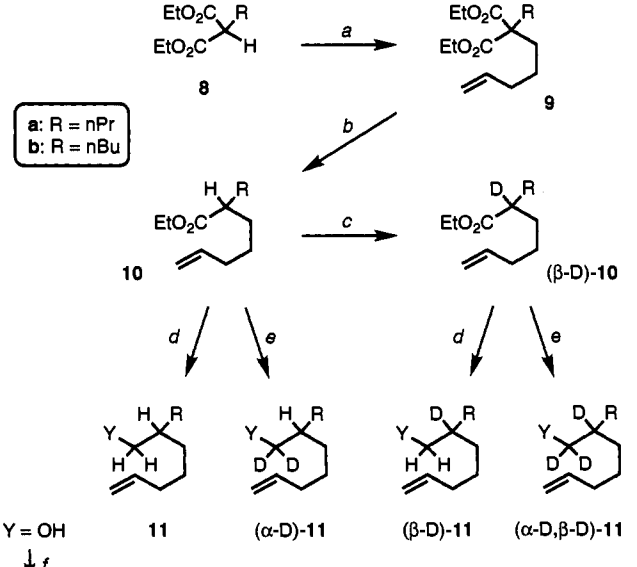

[a] Reaction conditions: (a) i, NaH, DMF; ii, 4-bromopentene (**b**: 99%); (b) H_2O, DMSO, LiCl, 180 °C (**a**: 90% from **8a**, **b**: 86%); (c) i, LDA; ii, *n*-BuLi; iii, D_2O (**a**: 89%, **b**: 92%); (d) i, $LiAlH_4$, ii, H_2O (90–98%); (e) i, $LiAlD_4$; ii, H_2O (92–95%); (f) NBS, PPh_3 (68–94%); (g) 4.0 equiv of Mg, (h) Cp_2TiCl_2.

(9) Clawson, L.; Soto, J.; Buchwald, S. L.; Steigerwald, M. L.; Grubbs, R. H. *J. Am. Chem. Soc.* **1985**, *107*, 3377.

(10) Krauledat, H.; Brintzinger, H.-H. *Angew. Chem., Int. Ed. Engl.* **1990**, *29*, 1412.

(11) (a) Röll, W.; Brintzinger, H.-H.; Rieger, B.; Zolk, R. *Angew. Chem., Int. Ed. Engl.* **1990**, *29*, 279. (b) Erker, G.; Nolte, R.; Aul, R.; Wilker, S.; Krüger, C.; Noe, R. *J. Am. Chem. Soc.* **1991**, *113*, 7594. (c) Lee, I.-M.; Gauthier, W. J.; Ball, J. M.; Iyengar, B.; Collins, S. *Organometallics* **1992**, *11*, 2115. (d) Mashima, K.; Nakamura, A. *J. Organomet. Chem.* **1992**, *428*, 49.

(12) Piers, W. E.; Bercaw, J. E. *J. Am. Chem. Soc.* **1990**, *112*, 9406.

(13) Young, J. R.; Stille, J. R. *J. Am. Chem. Soc.* **1992**, *114*, 4936.

(14) (a) Rigollier, P.; Young, J. R.; Fowley, L. A.; Stille, J. R. *J. Am. Chem. Soc.* **1990**, *112*, 9441. (b) Young, J. R.; Stille, J. R. *Organometallics* **1990**, *9*, 3022.

(15) A stereocenter at the δ-position was not incorporated into these simplified models because asymmetry at the β-position dominates the stereoselective chain end control process.

(16) Selection of the *n*-propyl and *n*-butyl substituents was made on the basis of reaction kinetics (methyl- and ethyl-substituted ligands resulted in cyclizations which were too rapid) and analytical procedures (optimum separation in GC analysis). Young, J. R. Ph.D. Thesis, Michigan State University, 1992.

Scheme 3. Intramolecular Insertion of **14**

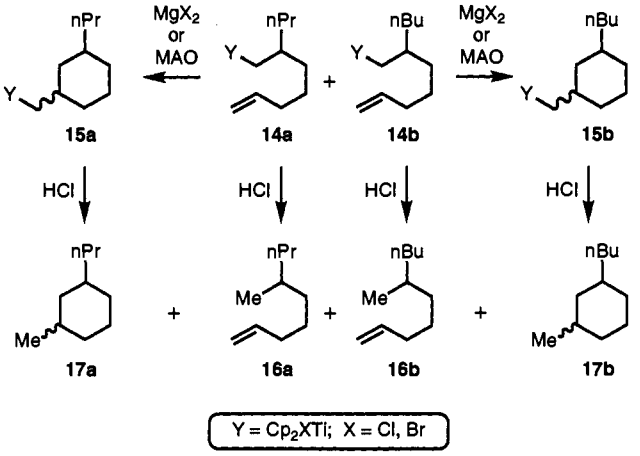

A number of selectively deuterated substrates (**14**) were prepared for this study through the divergent routes illustrated in Scheme 2. Alkylation of **8**, and subsequent deethoxycarboxylation of **9**,[17] provided an efficient route to **10**, which served as an intermediate in the preparation of all substrates. From **10**, substrates labeled at the β-position were prepared by deuteration of the corresponding enolate. Optimum deuterium incorporation was accomplished through sequential treatment of **10** with LDA, addition of *n*-BuLi to deprotonate the resulting *i*-Pr_2NH, and then addition of D_2O to produce (β-D)-**10** with >98% deuterium incorporation.[18] Reduction of **10** and (β-D)-**10** with $LiAlH_4$ gave alcohols **11** and (β-D)-**11**, which were converted to the corresponding bromides with NBS/PPh_3.[19] Similarly, treatment with $LiAlD_4$ and subsequent bromination provided routes to (α-D)-**12** and (α-D,β-D)-**12**.

Treatment of **12** with 4.0 equiv of Mg in Et_2O resulted in formation of the corresponding Grignard complex, and transmetalation to Cp_2TiCl_2 in CH_2Cl_2 generated the desired transition metal complex **14** *in situ* (Scheme 2). However, the Lewis acid formed as the product of transmetalation, MgX_2 (X = Br, Cl), promoted intramolecular insertion of the tethered alkene at ambient temperature to produce **15** (Scheme 3).[20] In this case, the combination of Cp_2TiRCl and MgX_2 resembled components of the heterogeneous $Cp_2TiCl_2/MgCl_2/TiCl_4/AlEt_3$ catalyst systems, which have been reported to produce isotactic formation of polypropylene.[21] Alternatively, the preparation of **14** could be accomplished with minimal conversion to **15** (<9%) when the Grignard complex was formed in THF, which deactivated the MgX_2 during the transmetalation procedure. Purification of the organometallic species was accomplished by solvent removal and extraction procedures to produce a THF- and MgX_2-free solution of **14** in toluene. Treatment of **14** with MAO in toluene resulted in efficient cyclization to **15** at –45 °C (Scheme 3).[22] Subsequent addition of 1-hexene (10.0 equiv) to this reaction mixture resulted in the insertion of 2–7 monomer units to generate the cyclohexane-capped oligomer, as determined by mass spectral analysis.

Table 1. Relative Rates for Competitive Cyclization of **14a** and **14b**[a]

		relative rates[b]	
entry	reaction **14a**:**14b**	MgX_2[c]	MAO[d]
1	α-H:α-H	1.14:1.00	1.33:1.00
2	α-D:α-D	1.19:1.00	1.43:1.00
3	α-H:α-D	1.43:1.00	1.26:1.00
4	α-D:α-H	1.00:1.09	1.51:1.00[e]
5	β-D:β-D	1.15:1.00	1.33:1.00
6	β-H:β-D	1.25:1.00	1.41:1.00
7	β-D:β-H	1.00:1.05	1.25:1.00
8	α-H,β-H:α-D,β-D	1.55:1.00	
9	α-D,β-D:α-H,β-H	1.00:1.20	

[a] Relative amounts determined by capillary GC (ref 23). [b] Unless noted otherwise, errors in these values are ±0.02 or ±0.03. [c] Reaction conditions: i, 1.0 equiv of **12a**, 1.0 equiv of **12b**, Mg, Et_2O, 25 °C; iii, Cp_2TiCl_2, toluene, –30 °C to 25 °C. X = Cl, Br. [d] Reaction conditions: i, 1.0 equiv of **12a**, 1.0 equiv of **12b**, Mg, THF, 35 °C; ii, Cp_2TiCl_2, CH_2Cl_2, –30 ° to 25 °C; iii, removal of THF and inorganic salts; iv, **14**, toluene, MAO, –45 °C. [e] Values = ±0.04.

Therefore, oligomeriation occurred under the same conditions used for cyclization, and the intramolecular insertion process serves as a suitable model for the analogous Ziegler–Natta polymerization systems.

Qualitatively, the different cyclization conditions produced visually distinct reaction mixtures. When promoted by MgX_2 in either CH_2Cl_2 or toluene, the reaction mixture was deep burgundy red in color, and both the intensity of the color and the formation of a precipitate made it difficult for light to pass through the mixture. In contrast, the reaction promoted by MAO in toluene was a transparent homogeneous solution that was orange-red in color. Both reaction mixtures were further distinguished from the $Cp_2TiRCl/[EtAlCl_2]_2$ catalyst mixtures in toluene, which were often dark brown to black.

The relative reactivity of equimolar amounts of **14a** and **14b** was examined through competitive cyclization reactions promoted by MgX_2 or MAO (Scheme 3). At regular time intervals, aliquots of the reactions were quenched by the addition of anhydrous HCl in Et_2O. The extent to which conversion of **14a** and **14b** to **15a** and **15b** had occurred was accurately determined by analysis of the quantity of **17a** and **17b** in the protonolysis mixture.[23] The competitive cyclization of **14a** and **14b** and that of (α-D)-**14a** and (α-D)-**14b** quantified effects due to the steric and electronic contributions of the *n*-propyl substituent relative to the *n*-butyl β-substituent prior to isotopic differentiation. These normalization values were then incorporated into the evaluation of subsequent cyclizations so that the actual deuterium isotope effects could be distinguished from the rate differences due to β-substituent variation.

In the case of MgX_2-promoted insertion, the relative rates for formation of **15a**/**15b** were found to be 1.14:1.00 (Table 1, entry 1).[24] The MAO-activated reaction produced more selective cyclization of substrates, in which the propyl substrate cyclized 33% more rapidly than the butyl.[25] The different selectivities

(17) (a) Krapcho, A. P.; Lovey, A. J. *Tetrahedron Lett.* **1973**, 957. (b) Krapcho, A. P.; Jahngen, E. G. E.; Lovey, A. J. *Tetrahedron Lett.* **1974**, *1091*. (c) Beckwith, A. L. J.; Easton, C. J.; Lawrence, T.; Serelis, A. K. *Aust. J. Chem.* **1983**, *36*, 545.

(18) Without the intermediate addition of *n*-BuLi, only 65 to 75% deuterium incorporation α to the carbonyl was achieved. Young, J. R. Ph.D. Thesis, Michigan State University, 1992.

(19) (a) Trippett, S. *J. Chem. Soc.* **1962**, 2337. (b) Bose, A. K.; Lai, B. *Tetrahedron Lett.* **1973**, 3937.

(20) During the transmetalation process, a mixture of Cp_2TiXR and MgX_2 is formed, in which the Br and Cl exchange to generate the various halogen combinations.

(21) (a) Soga, K.; Yanagihara, H. *Makromol. Chem., Rapid Commun.* **1987**, *8*, 273. (b) Soga, K.; Yanagihara, H. *Makromol. Chem.* **1988**, *189*, 2839. (c) Soga, K.; Park, J. R.; Uchino, H.; Uozumi, T.; Shiono, T. *Macromolecules* **1989**, *22*, 3824.

(22) These were found to be the optimum conditions for controlled cyclization of **14** with MAO. Variation in the amount of cocatalyst, reaction concentration, or reaction temperature resulted in a reactivity that was either too slow or too rapid for careful analysis of the insertion process.

(23) Product distributions and yields were determined by capillary gas chromatographic analysis of the quenched reaction mixture (HCl/Et_2O) with the use of dodecane as an internal standard and after correction for detector response.

(24) Ratios for relative rate differences were examined in the range of 3 to 30% conversion to cyclic products for MgX_2, and values represent the average of at least five experimental runs (see supplementary material). Beyond 30% conversion, the mass balance of **16** and **17** showed a significant drop, and accurate values for isotope effects could not be obtained. The combined mass balance for the conversion of **12** to (**16** + **17**) ranged from 70 to 80% yield, and the trans:cis ratio for the hydrolysis products (**16a** or **16b**) was the same (39:61 to 41:59) for each experimental run.

(25) Ratios for relative rate differences were examined in the range of 3 to 60% conversion to cyclic products for MAO (ratios did not fluctuate significantly up to 60% cyclization), and values represent the average of five to thirteen experimental runs. The trans:cis ratio for the hydrolysis products (**16a** or **16b**) was the same (59:41 to 61:39) for each experimental run, and yields for the conversion of **12** to (**16** + **17**) were between 75 and 85%. Variation in the concentration of MAO and **14** in toluene, from 0.05 to 0.3 M, did not affect the relative rates of cyclization for **14a** and **14b**.

Table 2. α-Deuterium Isotope Effects for Intramolecular Olefin Insertion of **14a** and **14b**[a]

$$\left[\frac{R^2}{(\alpha\text{-D})\text{-}R^1}\right]\cdot\left[\frac{R^1}{R^2}\right] = \boxed{\frac{k_H}{k_D}(R^1)} = \left[\frac{R^1}{(\alpha\text{-D})\text{-}R^2}\right]\cdot\left[\frac{(\alpha\text{-D})\text{-}R^2}{(\alpha\text{-D})\text{-}R^1}\right]$$

A B C D

				$\alpha\text{-}(k_H/k_D)\text{-}R^1$	
Lewis acid	R^1	R^2	substrate	A·B	C·D
MgX_2	*n*-Pr	*n*-Bu	**14a**	1.24 ± 0.03	1.20 ± 0.03
MgX_2	*n*-Bu	*n*-Pr	**14b**	1.25 ± 0.03	1.30 ± 0.02
MAO	*n*-Pr	*n*-Bu	**14a**	0.88 ± 0.04	0.88 ± 0.04
MAO	*n*-Bu	*n*-Pr	**14b**	0.95 ± 0.04	0.95 ± 0.04

[a] Calculated from the values in Table 1.

Table 3. β-Deuterium Isotope Effects for Intramolecular Olefin Insertion of **14a** and **14b**[a]

$$\left[\frac{R^2}{(\beta\text{-D})\text{-}R^1}\right]\cdot\left[\frac{R^1}{R^2}\right] = \boxed{\frac{k_H}{k_D}(R^1)} = \left[\frac{R^1}{(\beta\text{-D})\text{-}R^2}\right]\cdot\left[\frac{(\beta\text{-D})\text{-}R^2}{(\beta\text{-D})\text{-}R^1}\right]$$

A B C D

				$\beta\text{-}(k_H/k_D)\text{-}R^1$	
Lewis acid	R^1	R^2	substrate	A·B	C·D
MgX_2	*n*-Pr	*n*-Bu	**14a**	1.09 ± 0.02	1.09 ± 0.02
MgX_2	*n*-Bu	*n*-Pr	**14b**	1.10 ± 0.02	1.10 ± 0.02
MAO	*n*-Pr	*n*-Bu	**14a**	1.06 ± 0.04	1.06 ± 0.04
MAO	*n*-Bu	*n*-Pr	**14b**	1.06 ± 0.04	1.06 ± 0.04

[a] Calculated from the values in Table 1.

observed for MgX_2 and MAO paralleled the difference in reaction temperature at which the MgX_2 (25 °C) and MAO (−45 °C) reactions were performed. As observed for **6** (eq 2), the trans/cis ratios of **17a** and **17b** were dependent upon the cyclization conditions (40:60 for MgX_2, 60:40 for MAO), with the greater selectivity for **6** due to the increased steric influence of the isopropyl substituent.[13,24,25] Competitive cyclization of (α-D)-**14a** and (α-D)-**14b** promoted by MgX_2 and MAO produced slightly greater rate discrimination in substrate cyclization to give values of 1.19:1.00 and 1.43:1.00, respectively, accompanied by unaffected cis/trans product ratios (Table 1, entry 2).

α-Deuterium Isotope Effects. From the results of the competitive cyclization of **14a** and (α-D)-**14b** as well as (α-D)-**14a** and **14b** (Table 1, entries 3 and 4), the differences in reaction outcome as a result of Lewis acid variation became very apparent. Deuteration at the α-position slowed insertion for MgX_2-promoted cyclization, while MAO-promoted cyclization was *enhanced* upon α-deuteration. Although the significantly different ratios observed in entries 3 and 4 immediately suggested isotope effects at the α-position, correction for the substituent effects was necessary. From these relative rates, the k_H/k_D for **14a** could be determined through two independent calculations, which helped to ensure the internal consistency of the values obtained (Table 2).

Normalization of the relative rate for MgX_2-promoted cyclization of (α-D)-**14a** and **14b** was accomplished by taking the product of **14b**/(α-D)-**14a** (1.09, Table 1, entry 4) and the normalization factor **14a**/**14b** (1.14, Table 1, entry 1) to give a k_H/k_D of 1.24 ± 0.03 for **14a** (**A·B**, Table 2). Similarly, the product of **14a**/(α-D)-**14b** and (α-D)-**14b**/(α-D)-**14a** generated a comparable k_H/k_D for **14a** of 1.20 ± 0.03 (**C·D**, Table 2). The average of these results gave a k_H/k_D value of 1.22 for **14a**. Values for the k_H/k_D of **14b**, 1.25 and 1.30, were obtained in the same manner. These values were slightly larger and led to an average k_H/k_D of 1.27 for **14b**.

The competitive reaction of **14a** and (α-D)-**14b** and the competition between (α-D)-**14a** and **14b** produced unexpected results when olefin insertion was promoted by MAO (Table 1, entries 3 and 4). On the basis of the different relative reaction rates, which magnified the actual isotope effect by a factor of 2, an inverse α-deuterium isotope effect was observed. With the use of either normalization factor, the values obtained for the k_H/k_D of **14a** were both 0.88 ± 0.04, and the analogous value for the k_H/k_D of **14b** was 0.95 ± 0.04 (Table 2). Due to the lesser degree of the inverse k_H/k_D for the butyl-substituted ligand than for the propyl, these values suggested a trend in which the isotope effects are stronger as the size of the β-substituent decreases and therefore could be even greater during the propagation of polypropylene.

β-Deuterium Isotope Effects. Evidence for β-hydrogen interactions has been obtained in related systems through X-ray diffraction analysis of ethyl complexes of titanium,[26] zirconium,[27] and cobalt,[28] in which agostic interaction of a β-hydrogen with the electron-deficient metal center was observed. These interactions have been most commonly used to describe the resting state of an active catalyst, or the prerequisite complex for β-hydrogen elimination/chain termination in Ziegler–Natta polymerization.[8,10,29] However, agostic interactions with the β-hydrogen have also been suggested as a part of chain propagation.[27,28]

With the use of substrates labeled in the β position, participation of the β-hydrogen in the rate-determining step of MgX_2-promoted olefin insertion was examined. A normalization value of 1.15 ± 0.01 was obtained for (β-D)-**14a**/(β-D)-**14b** (Table 1, entry 5), and this value was used as the second correction factor in combination with the **14a**/**14b** value of 1.14 ± 0.01 (Table 1, entry 1). From the experimental data in entries 6 and 7, which magnified the differences due to C–H interactions, a k_H/k_D of >1.0 was evident (Table 1). Normalization of the observed values through both independent routes produced the same k_H/k_D of 1.09 ± 0.02 for **14a** (Table 3). Similarly, a value of 1.10 ± 0.02 was obtained for the k_H/k_D of **14b**. The k_H/k_D values obtained for **14a** and **14b** provided experimental support that β-hydrogen participation is involved in the chain propagation step for Ziegler–Natta polymerization of α-olefins.

Studies of the MAO-promoted cyclization produced similar results to reveal a kinetic isotope effect for the β-hydrogen. In addition to the normalization value already acquired for **14a**/**14b** (1.33 ± 0.03), a second correction factor of 1.33 ± 0.02 was obtained in the form of (β-D)-**14a**/(β-D)-**14b** (Table 1, entry 5). Comparison of the relative reaction rates for entries 6 and 7 revealed inhibition of cyclization upon deuteration at the β-position, and correction of the comparative rates for the different substituent effects gave the same k_H/k_D value of 1.06 ± 0.04 for substrate **14a** (Table 3). A value of 1.06 ± 0.04 was also obtained for the k_H/k_D of **14b**, which further substantiated the presence of a small deuterium isotope effect for this catalyst/cocatalyst model.

Cooperative Activation by α- and β-Hydrogens. With the observation of both α- and β-isotope effects for the intramolecular olefin insertion into the titanium–carbon bonds of **14a** and **14b**, the interactive relationship between these effects was examined. The relative rates observed for **14a**/(α-D,β-D)-**14b** and (α-D,β-D)-**14a**/**14b** were 1.55:1.00 and 1.00:1.20, respectively, and these values illustrated an even greater difference than those from entries 3 and 4 in Table 1. Correction for the substituent effects produced k_H/k_D values of 1.37 and 1.36 ± 0.02 for **14a** and **14b**, respectively (Table 4). These values represent a cooperative or additive effect of the α- and β-hydrogen activation. Because the small inverse α-isotope effect was expected to simply offset the contribution

(26) (a) Dawoodi, Z.; Green, M. L. H.; Mtetwa, V. S. B.; Prout, K. *J. Chem. Soc., Chem. Commun.* **1982**, 802. (b) Dawoodi, Z.; Green, M. L. H.; Mtetwa, V. S. B.; Prout, K.; Schultz, A. J.; Williams, J. M.; Koetzle, T. F. *J. Chem. Soc., Dalton Trans.* **1986**, 1629.

(27) Jordan, R. F.; Bradley, P. K.; Baenziger, N. C.; LaPointe, R. E. *J. Am. Chem. Soc.* **1990**, *112*, 1289.

(28) (a) Brookhart, M.; Green, M. L. H.; Pardy, R. B. A. *J. Chem. Soc., Chem. Commun.* **1983**, 691. (b) Cracknell, R. B.; Orpen, A. G.; Spencer, J. L. *J. Chem. Soc., Chem. Commun.* **1984**, 326. (c) Schmidt, G. F.; Brookhart, M. *J. Am. Chem. Soc.* **1985**, *107*, 1443. (d) Brookhart, M.; Volpe, A. F., Jr.; Lincoln, D. M.; Horváth, I. T.; Millar, J. M. *J. Am. Chem. Soc.* **1990**, *112*, 5634.

(29) Kaminsky, W.; Hahnsen, H. *Advances in Polyolefins*; Seymour, R. B., Cheng, T., Eds.; Plenum: New York, 1987; p 361.

Table 4. Cooperative α- and β-Deuterium Isotope Effects for Intramolecular Olefin Insertion of **14a** and **14b**[a]

$$\left[\frac{R^2}{(\alpha,\beta\text{-D})\text{-}R^1}\right] \cdot \left[\frac{R^1}{R^2}\right] = \boxed{\frac{k_H}{k_D}(R^1)}$$

A B

	α,β-(k_H/k_D)-R^1			
Lewis acid	R^1	R^2	substrate	A·B
MgX_2	*n*-Pr	*n*-Bu	**14a**	1.37 ± 0.02
MgX_2	*n*-Bu	*n*-Pr	**14b**	1.36 ± 0.02

[a] Calculated from the values in Table 1.

of the minor isotope effect at the β-position, analogous studies with MAO were not examined. In line with the data obtained for the MAO-promoted insertion, examination of the relative reactivity of $CH_2{=}CH_2$ *versus* $CD_2{=}CD_2$ did not produce a measurable isotope effect for the $Cp_2TiCl_2/EtAlCl_2$ catalyst system, possibly due to the cancellation of the α and β effects.[30]

Mechanistic Implications. Several important features of the active catalyst/cocatalyst species in Ziegler–Natta polymerizations have already been firmly established. The extensive structural network (-X-M-X-M-X-M-; M = metal; X = halogen, oxygen) present in both heterogeneous (MgX_2) and homogeneous (MAO) cocatalysts is of primary importance for the effectiveness of these cocatalysts (Scheme 4).[31] The Lewis acidic properties of the cocatalyst serve to activate the catalyst through generation of an electron-deficient transition metal center such as **18** or **19**.[32] Once activation has occurred, the -X-M-X-M-X-M- cocatalyst networks function as delocalized counteranions, which interact with the catalyst to stabilize the cationic transition metal complex and to maintain catalyst activity through increased catalyst lifetime.[33]

Stereoselective polymer formation then occurs as a result of subtle effects of catalyst–cocatalyst–ligand interactions. These ligand interactions were observed in the cyclization of **14**, where the different Lewis acid reaction conditions resulted in contrasting trans/cis stereoselectivities for **17**. Closer examination of potential ligand participation revealed the kinetic isotope effects summarized in Figure 1. In these studies, participation of the β-hydrogen was of comparable magnitude for both MgX_2 and MAO and did not serve to distinguish the actions of the Lewis acids. The most dramatic mechanistic differences in Lewis acid function were evident from the opposing k_H/k_D values observed for the α-hydrogen.

Due to the apparent dependence of olefin insertion on the cocatalyst, α-hydrogen interactions could occur either with the transition metal (**20**) or with the MgX_2 cocatalyst (**23** or **26**). In the case of **26**, structural evidence for the bridging of the alkyl chain between the catalyst and cocatalyst (**26** through **28**) has been provided in related zirconium species.[34] As a result of any of these interactions, the titanium–carbon bond would have increased reactivity toward olefin insertion due to an increase in favorable orbital geometry of the α-carbon.[8]

Scheme 4. Olefin Insertion: Possible Origins of Activation/Stereocontrol[a]

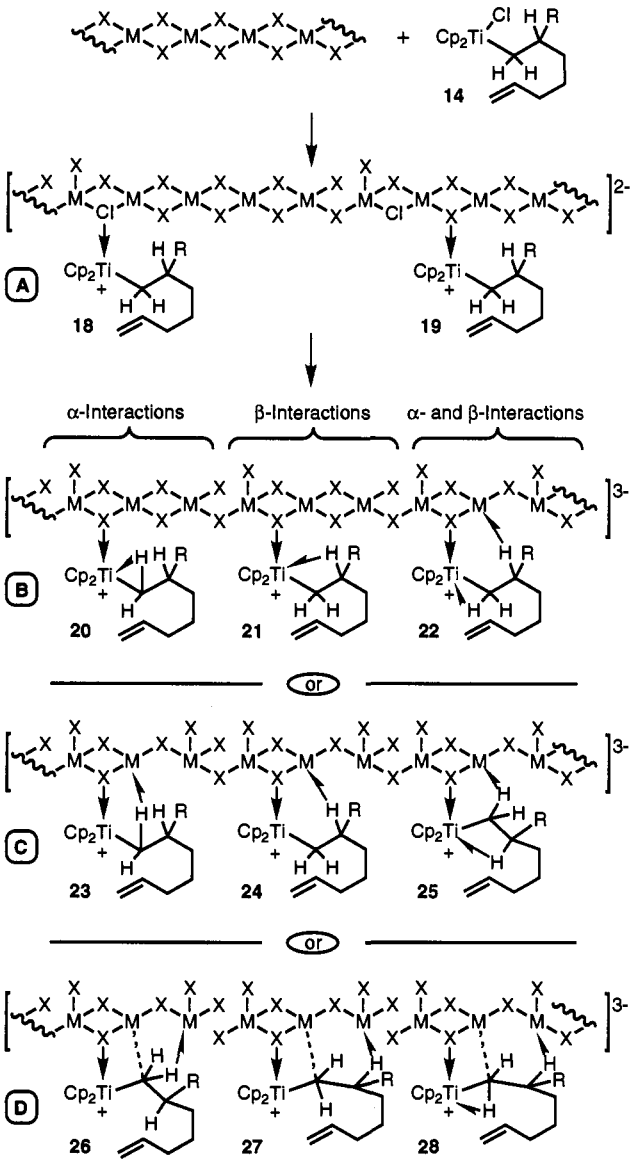

[a] **A**: catalyst activation. **B**: agostic interaction with transition metal. **C**: agostic interaction with cocatalyst. **D**: combined bridging alkyl ligand and agostic interaction with cocatalyst.

Interestingly, the *trans*-**16a**/*cis*-**16a** ratio produced by radical cyclization of **12a** was the same as that for the MgX_2-promoted cyclization (42:58). Coupled with the k_H/k_D values typically observed for the secondary isotope effects in free radical processes,[35] the possibility of bond homolysis, cyclization, and recombination with the metal also arises. However, free radical cyclization conditions (Bu_3SnH, AIBN, C_6H_6, 80 °C, 0.01 M) produced only 36% conversion of **12a** to **16a**. In contrast, the MgX_2-promoted cyclization could be driven to 88% conversion under less favorable conditions for intramolecular bond formation (0.33 M).

(30) (a) Grigoryan, E. A.; D'yachkovskii, F. S.; Shilov, A. Y. *Polym. Sci. USSR (Engl. Trans.)* **1965**, *7*, 158. (b) Reichert, V. K. H.; Schubert, E. *Die Makromol. Chem.* **1969**, *123*, 58. (c) Soto, J.; Steigerwald, M. L.; Grubbs, R. H. *J. Am. Chem. Soc.* **1982**, *104*, 4479.

(31) In the absence of such a structural framework, as in the case of $[EtAlCl_2]_2$, propylene dimerization occurred. Goodall, B. L. *Transition Metals and Organometallics as Catalysts for Olefin Polymerization*; Kaminsky, W., Sinn, H., Eds.; Springer-Verlag: Berlin, 1988; p 362.

(32) For examples of cationic polypropylene catalysts, see the following. (a) Ti: Bochmann, M.; Jaggar, A. J.; Nichols, J. C. *Angew. Chem., Int. Ed. Engl.* **1990**, *29*, 780. (b) Zr: Jordan, R. F. *Adv. Organomet. Chem.* **1991**, *32*, 325. (c) Yang, X.; Stern, C. L.; Marks, T. J. *J. Am. Chem. Soc.* **1991**, *113*, 3623.

(33) Coordination of cocatalysts in polymerization systems has been structurally confirmed: (a) Eisch, J. J.; Piotrowski, A. M.; Brownstein, S. K.; Gabe, E. J.; Lee, F. L. *J. Am. Chem. Soc.* **1985**, *107*, 7219. (b) Hlatky, G. G.; Turner, H. W.; Eckman, R. R. *J. Am. Chem. Soc.* **1989**, *111*, 2728. (c) Sishta, C.; Hathorn, R. M.; Marks, T. J. *J. Am. Chem. Soc.* **1992**, *114*, 1112. (d) Horton, A. D.; Frijns, J. H. G. *Angew. Chem., Int. Ed. Engl.* **1991**, *30*, 1152.

(34) (a) Kaminsky, W.; Kopf, J.; Thirase, G. *Liebigs Ann. Chem.* **1974**, 1531. (b) Kaminsky, W.; Kopf, J.; Sinn, H.; Vollmer, H.-J. *Angew. Chem., Int. Ed. Engl.* **1976**, *15*, 629. (c) Lvovsky, V. E.; Fushman, E. A.; D'yachkovsky, F. S. *J. Mol. Catal.* **1981**, *10*, 43. (d) Waymouth, R. W.; Potter, K. S.; Schaefer, W. P.; Grubbs, R. H. *Organometallics* **1990**, *9*, 2843. (e) Erker, G.; Albrecht, M.; Kruger, C.; Werner, S.; Binger, P.; Langhauser, F. *Organometallics* **1992**, *11*, 3517.

(35) (a) Streitwieser, A., Jr.; Jagow, R. H.; Fahey, R. C.; Suzuki, S. *J. Am. Chem. Soc.* **1958**, *80*, 2326. (b) Strausz, O. P.; Safarik, I.; O'Callaghan, W. B.; Gunning, H. E. *J. Am. Chem. Soc.* **1972**, *94*, 1828. (c) Lowry, T. H.; Richardson, K. S. *Mechanism and Theory in Organic Chemistry*, 3rd ed.; Harper and Row Publishers: New York, 1987; p 240.

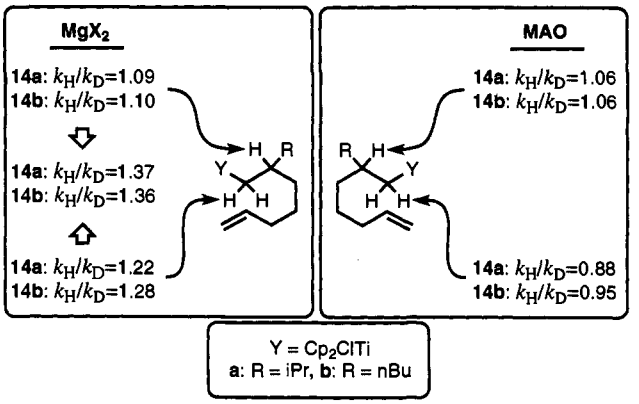

Figure 1. Summary of k_H/k_D values for activation of **14** with MgX_2 and methylaluminoxane (MAO).

In contrast to results obtained with MgX_2, MAO-activated insertion produced an inverse isotope effect at the α-position. The occurrence of an inverse isotope effect indicates the possibility of a ground state α-agostic interaction, from which the α-D species would demonstrate greater reactivity. Alternatively, a hybridization change at the α-carbon, through increased p character and a decrease in D–C–D bond angle in the transition state, could also account for an inverse isotope effect.[35] During the insertion process, transfer to the alkyl group occurs with retention of stereochemistry at the α-carbon,[2a] which would proceed along the edge of the trigonal-bipyramidal geometry (H–C(α)–H changes from 109° to 90°).

The nature of the Lewis acid metal was of obvious significance in producing divergent mechanistic features.[36] However, the ionic strength of the solvent or the temperature at which these reactions were performed (MAO, toluene, –45 °C; MgX_2, CH_2Cl_2/Et_2O, 25 °C) could play an integral role in the different reaction outcomes. In similar systems, a decrease in temperature from 25 to –10 °C resulted in an increase in the k_H/k_D values from 1.19:1.00 to 1.26:1.00 for the scandium-mediated cyclization,[12] and the closely related titanocene/MAO systems have produced more significant differences. At –50 °C, a representative titanocene/MAO system produced isotactic polypropylene (σ = 0.80), while a preference for syndiotactic polypropylene (σ = 0.35) resulted at 10 °C (σ = index of tacticity: 1.00 = 100% isotactic, 0.00 = 100% syndiotactic).[37] Similarly, an increase in temperature has produced a general decrease in polymer stereoregularity for other zirconium-based catalysts.[11,38] Importantly, the mechanistic work reported for **3**, with which these results are compared, was performed at –5 °C (Scheme 1).[10] On the basis of these observations, the temperature dependence of stereoselective polymer formation could be a key factor in changes in reaction mechanism.

Although involvement of the β site does not serve to distinguish the MgX_2 and MAO systems, this feature may be important for activation of the alkyl ligand toward olefin insertion. When compared to the magnitude of the kinetic isotope effects observed for the α-agostic interactions proposed for zirconium[10] and scandium catalysts,[12] the values of interactions with the β-hydrogen are smaller. However, coordination of the hydridic β-hydrogen in an agostic interaction does not require the same degree of geometric change at the β-carbon as is necessary for agostic interaction of the α-position and thus would produce a smaller isotope effect for comparable activation. On the basis of these results, a β-agostic effect could occur with either the titanium (**21**) or the cocatalyst center (**24** or **27**, M = Mg or Al). Such interactions represent a transition state for β-hydride elimination and produce a state in which the titanium–carbon bond is weakened and thus activated toward olefin insertion.

Scheme 5. Potential Stereocontrol Resulting from β-Hydrogen Interactions

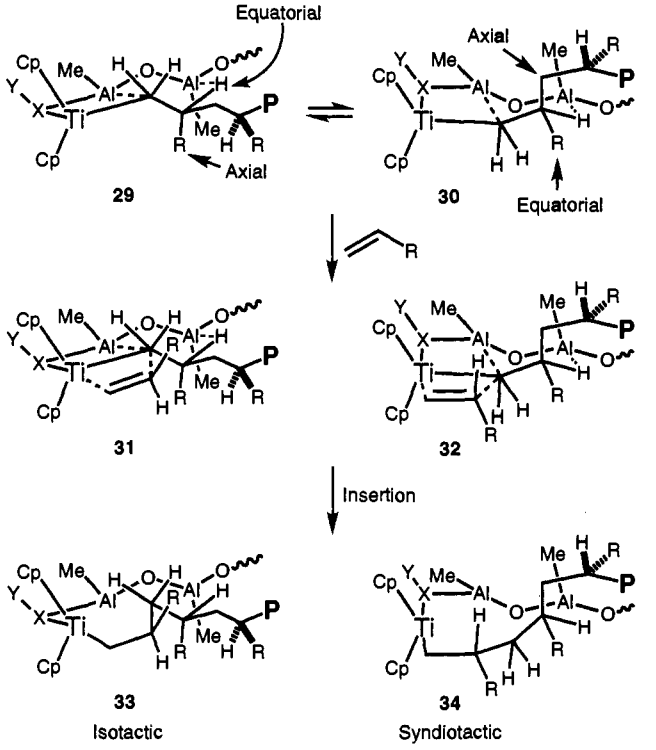

The involvement of β-hydrogen interactions in olefin insertion gives rise to conformationally restricted transition states and can be used to account for stereoregular MAO-promoted polymerization of α-olefins. This model includes a β-hydrogen interaction, which results in a six-membered C(α)–C(β)–H(β)–Al–O–Al ring in the olefin insertion transition state, and stereoselective product formation occurs as a result of the substituent orientation at the β-carbon (R *versus* CH_2CHRP, Scheme 5). When R is smaller in size than the propagating polymer chain, as in propylene polymerization (R = Me), then R will be directed toward the axial position (**29**) rather than the equatorial orientation (**30**) relative to the six-membered ring illustrated. In the case of propylene, approach of the olefin with the methyl group opposite the more sterically imposing polymer chain (**31**) would produce isotactic polymer formation (**33**) through this chain end control process (CH_3 *versus* CH_2CHCH_3P).[2,39] In accord with this model, a decrease in the steric differentiation between the alkyl side chain and the polymer chain, such as the polymerization of 1-butene (CH_2CH_3 *versus* CH_2CHRP), produced only moderately isotactic polymer.[39] Elimination of any significant steric

(36) Although aluminum and magnesium species have been reported to cyclize with tethered alkene functionality, cyclization with the MgX_2 and aluminum-based cocatalyst systems was demonstrated to occur at titanium. Under the conditions of MgX_2-promoted reaction, the addition of 0.50 equiv of Cp_2TiCl_2 to **13a** produced only 50% cyclization of the ligand, while the addition of 0.5 equiv of MgX_2 to **14** led to >75% ligand cyclization. Mg cyclization: (a) St. Denis, J.; Oliver, J. P.; Dolzine, T. W.; Smart, J. B. *J. Organomet. Chem.* **1974**, *71*, 315 (five-membered ring). (b) Richey, H. G., Jr.; Veale, H. S. *J. Am. Chem. Soc.* **1974**, *96*, 2041 (five-membered ring). A related reaction, in which **14a** (Y = $TiXCp_2$) and **14c** (Y = $AlCl_2$) were mixed, again produced only cyclization of the ligand on titanium. Cyclization of tethered alkenes on aluminum has generated five- and six-membered ring products at temperatures exceeding 25 °C. (c) Stefani, A. *Helv. Chim. Acta* **1974**, *57*, 1346 (five-membered ring). (d) Rienäcker, R.; Schwengers, D. *Liebigs Ann. Chem.* **1977**, 1633 (six-membered ring).

(37) Erker, G.; Fritze, C. *Angew. Chem., Int. Ed. Engl.* **1992**, *31*, 199.

(38) (a) Rieger, B.; Mu, X.; Mallin, D. T.; Rausch, M. D.; Chien, J. C. W. *Macromolecules* **1990**, *23*, 3559. (b) Chien, J. C. W.; Sugimoto, R. *J. Polym. Sci., Part A-1* **1991**, *29*, 459. (c) Babu, G. N.; Newmark, R. A.; Cheng, H. N.; Llinas, G. H.; Chien, J. C. W. *Macromolecules* **1992**, *25*, 7400. (d) Rieger, B. *J. Organomet. Chem.* **1992**, *428*, C33. (e) Rieger, B.; Jany, G.; Fawzi, R.; Steimann, M. *Organometallics* **1994**, *13*, 647.

(39) (a) Zambelli, A.; Ammendola, P.; Grassi, A.; Longo, P.; Proto, A. *Macromolecules* **1986**, *19*, 2703. (b) Ammendola, P.; Pellecchia, C.; Longo, P.; Zambelli, A. *Gazz. Chim. Ital.* **1987**, *117*, 65. (c) Zambelli, A.; Ammendola, P. *Transition Metals and Organometallics as Catalysts for Olefin Polymerization*; Kaminsky, W., Sinn, H., Eds.; Springer-Verlag: Berlin, 1988; p 329.

bias, through the use of 4-methyl-1-pentene as a monomer (CH_2-$CHMe_2$ *versus* CH_2CHRP), resulted in the formation of atactic polymer.

Combination of both α- and β-hydrogen interactions leads to an interesting range of mechanistic possibilities. In the case of MgX_2, which produced k_H/k_D values in the range of 1.22 to 1.28 for α-hydrogens and k_H/k_D values from 1.09 to 1.10 for β-hydrogens, simultaneous activation could occur through structures **22**, **25**, or **28**. Alternatively, the α-hydrogen interaction in the MAO-promoted reaction could serve as a ground state species, which would block olefin insertion. This feature, coupled with a change in hybridization of the α-carbon during insertion, would both contribute to an inverse α-isotope effect. The resulting k_H/k_D of 1.06 at the β-position could reflect insertion through structures **21**, **24**, or **27**.

Agostic interactions of β-hydrogens contribute to the observed Lewis acid cocatalyst dependence and the process of chain end control. Similarly, the concept of chain participation in the transition state of olefin insertion can be used to explain ligand effects on the rate of chain propagation. For example, catalyst systems of the type Cp_2TiRCl that contain a ligand with a β-H ($R = CH_2CH_3$) produced much faster initial olefin insertion than when β-hydrogens were absent (R = Me, Ph, CH_2CMe_3, and Bn).[40] In addition, the subsequent rate of propagation was faster than initiation for catalysts in which R = Me or Ph.[40]

Conclusions

These findings represent the first evidence for α-hydrogen participation in the rate-determining step of α-olefin insertion for titanium-based Ziegler–Natta catalyst systems as well as for any system which modeled a propagating α-olefin polymer chain of the heterogeneous MgX_2 and homogeneous MAO catalyst systems. When cyclization was promoted by MgX_2, the average k_H/k_D values obtained for the α-hydrogen participation, 1.22 and 1.28 ± 0.03, were comparable to the previously reported zirconium[10] and scandium[12] systems that modeled polyethylene propagation. These values are consistent with α-agostic interactions or secondary isotope effects due to hyperconjugation with the proposed intermediate titanium cation. The inverse isotope effects obtained for the MAO α-hydrogen interactions, 0.88 and 0.95 ± 0.03, were in sharp contrast to those of the previously reported for models of polyethylene propagation. The differences in α-hydrogen participation accounted for the contrasting trans/cis stereochemistry produced upon cyclization of **6** and **14** and for the different stereochemical outcomes of polymer formation by titanium and zirconium catalysts.

Due to the unique nature of poly α-olefin models, slight participation of the β-hydrogen was detected for the first time in these Ziegler–Natta catalyst/cocatalyst model systems. The magnitude of the β-hydrogen interactions in the rate-determining step of the carbon–carbon bond formation process ($k_H/k_D = 1.09$ and 1.10 ± 0.03) was less than those of the α-hydrogen interactions with MgX_2 and occurred in concert with the α-hydrogen interactions. Similar β-hydrogen effects ($k_H/k_D = 1.06 \pm 0.03$) were observed with the use of MAO as the cocatalyst.

Experimental Section

General Methods. All reactions were conducted under nitrogen or argon atmospheres. THF, Et_2O, toluene, and benzene were distilled from sodium/benzophenone prior to use. Hexane was stirred over sulfuric acid, and after 5 days, the hexane was washed sequentially with H_2O and saturated aqueous $NaHCO_3$, dried ($CaCl_2$), and distilled from sodium/benzophenone/tetraglyme. The Mg used for formation of the Grignard reagents was activated prior to use by washing with 10% HCl, H_2O, acetone, and finally Et_2O. The turnings were then flame dried *in vacuo* and stored in a desiccator. 4-Bromo-1-pentene[41] and MAO[42] were prepared according to published procedures.

NMR spectra were obtained on a Varian Gemini 300 or a VXR-300 instrument with $CDCl_3$ as solvent. Signals are reported in units of ppm relative to $C(^1H)Cl_3$ or $^{13}CHCl_3$. Analytical gas chromatography (GC) was performed with a 50 m RSL200 column (5% methyl phenyl silicone equivalent to SE-54 or DB-5).

Diethyl 2-(4-Pentenyl)-2-propylpropanedioate (9a).[43] NaH (1.89 g, 79 mmol) was suspended in DMF (61 mL), **8a** (14.78 g, 73 mmol) was added dropwise at room temperature over a 15 min period, and the resulting solution was stirred until all of the NaH was consumed (approximately 45 min). At this point, 4-bromo-1-pentene (10.0 g, 67 mmol) was added slowly, and the reaction was heated at 65 °C until the bromide was consumed (3–12 h). Upon completion of the alkylation, the mixture was cooled to 0 °C and diluted with H_2O (120 mL), and the aqueous layer was extracted with Et_2O (3 × 60 mL). The organic extracts were washed with H_2O (3 × 30 mL) followed by saturated aqueous NaCl. The Et_2O layer was dried ($MgSO_4$), concentrated, and carried on without further purification.

Ethyl 2-Propyl-6-heptenoate (10a). Crude diester **9a** (26.3 g, 97 mmol) and LiCl (7.9 g, 186 mmol) were taken up in DMSO (196 mL), and H_2O (1.8 mL, 100 mmol) was added. The mixture was heated in an oil bath at 180 °C until reaction was complete by NMR analysis (8–12 h). Dilution with H_2O (120 mL) was followed by extraction with Et_2O (3 × 60 mL). The organic layers were combined and washed with H_2O (2 × 30 mL), saturated aqueous $NaHCO_3$ (2 × 30 mL), and saturated aqueous NaCl (2 × 30 mL). The Et_2O layer was then dried ($MgSO_4$), concentrated, and distilled *via* Kugelrohr (oven temperature 80–90 °C, <1 Torr) to give **10a** (17.68 g, 90 mmol) in 90% yield from **8a**: ^1H NMR (300 MHz, $CDCl_3$) δ 0.85 (t, J = 7.3 Hz, 3 H), 1.20–1.59 (m, 12 H), 2.00 (q, J = 7.3 Hz, 2 H), 2.30 (m, 1 H), 4.09 (q, J = 7.3 Hz, 2 H), 4.90 (m, 1 H), 4.95 (m, 1 H), 5.74 (ddt, J = 17.0, 10.1, 7.3, 1 H); ^{13}C NMR (75 MHz, $CDCl_3$) δ 14.0, 14.3, 20.6, 26.7, 31.9, 33.6, 34.7, 45.5, 60.0, 114.6, 138.5, 176.5; IR (film) 3078, 2959, 2937, 2874, 1734, 1641, 1460, 1379, 1177, 911 cm^{-1}.

Ethyl 2-Propyl-2-deuterio-6-heptenoate ((β-D)-10a). A solution of LDA was prepared by adding *n*-BuLi (2.5 M in hexanes, 17.0 mL, 43 mmol) to a 0 °C solution of *i*-Pr_2NH (6.5 mL, 46 mmol) in THF (55 mL). Stirring was continued for 30 min, and the mixture was cooled to −78 °C. Compound **10a** (7.64 g, 39 mmol) was added dropwise to the LDA solution and stirred for 50 min. *n*-BuLi (23.2 mL, 2.5 M in hexanes, 58 mmol) was added to the reaction mixture at −78 °C (to deprotonate *i*-Pr_2NH), and the mixture was stirred for 30 min. The reaction was then quenched with D_2O (25 mL), the solution was warmed to ambient temperature, and the aqueous layer was extracted with Et_2O (3 × 30 mL). The Et_2O solution was washed with 1 M HCl (2 × 30 mL), saturated aqueous $NaHCO_3$ (2 × 60 mL), and saturated aqueous NaCl (60 mL), dried ($MgSO_4$), filtered, and concentrated to an oil. The crude oil was distilled under reduced pressure (oven temperature 70–80 °C, <1 Torr) to give (β-D)-**10a** (6.8 g, 35 mmol, 89% yield): ^1H NMR (300 MHz, $CDCl_3$) δ 0.86 (t, J = 7.1 Hz, 3 H), 1.22 (t, J = 7.1 Hz, 3 H), 1.28–1.46 (m, 6 H), 1.50–1.63 (m, 2 H), 2.00 (q, J = 6.6 Hz, 2 H), 4.09 (q, J = 7.1 Hz, 2 H), 4.90 (m, 1 H), 4.96 (m, 1 H), 5.73 (ddt, J = 17.1, 10.4, 6.6 Hz, 1 H); ^{13}C NMR (75 MHz, $CDCl_3$) δ 14.0, 13.9, 20.1, 26.2, 31.4, 33.2, 34.1, 59.5, 114.2, 138.1, 176.0; IR (film) 3079, 2959, 2934, 2873, 2860, 2145, 1732, 1641, 1460, 1035, 911 cm^{-1}.

General Procedure for $LiAlH_4$ or $LiAlD_4$ Reduction of Esters to 11. The reducing reagent (1.1 equiv of $LiAlH_4$ or $LiAlD_4$) was suspended in Et_2O (0.5 M) at 0 °C, and a solution of **10** in Et_2O (1.0 equiv, 0.3 M) was added to the $LiAlH_4$ suspension over a period of 30 min. Once addition was complete, the ice bath was removed, and the mixture was stirred at room temperature until the reaction was complete as determined by NMR analysis. The reaction mixture was cooled to 0 °C and the reaction was quenched by the slow sequential addition of H_2O (1.0 mL/g reducing reagent), 15% NaOH (1.0 mL/g reducing reagent), and H_2O (3.0 mL/g reducing reagent) and stirred until all of the solids turned white. At this time, $MgSO_4$ was added, and the mixture was stirred for an additional 30 min. The Et_2O was decanted from the solids, which were washed thoroughly with Et_2O, and the combined organic fractions were concentrated and distilled *via* Kugelrohr (over temperature 70–80 °C, <1 Torr) to provide the desired alcohol.

11a: 13.21 g, 85 mmol, 96% yield; ^1H NMR (300 MHz, $CDCl_3$) δ 0.87 (t, J = 6.8 Hz, 3 H), 1.13-1.50 (m, 10 H), 1.98–2.05 (m, 2 H), 3.49 (d, J = 5.4 Hz, 2 H), 4.92 (m, 1 H), 4.96 (m, 1 H), 5.77 (ddt, J = 17.0, 10.2, 6.7 Hz, 1 H); ^{13}C NMR (75 MHz, $CDCl_3$) δ 14.4, 20.0, 26.1, 30.4,

(40) Waters, J. A.; Mortimer, G. A. *J. Polym. Sci., Part A-1* **1972**, *10*, 1827.

(41) Kraus, G.; Landgrebe, K. *Synthesis* **1984**, 885.

(42) Kaminsky, W.; Hähnsen, H. U.S. Patent 4 544 762, October 1, 1985. Example 1.

(43) Due to the parallel series of reactions for **12a** and **12b**, and the similar spectral data, only the data for the *n*-propyl series (**a**) are reported here.

33.2, 34.1, 40.2, 65.6, 114.4, 138.9; IR (film) 3337, 3079, 2958, 2930, 2872, 1641, 1460, 1040, 993, 911 cm^{-1}.

(α-D)-**11a**: 5.58 g, 35 mmol, 94% yield. Spectral data were similar to those obtained for **11a** with the following exceptions: ^1H NMR (300 MHz, $CDCl_3$) δ 3.49 was absent; ^{13}C NMR (75 MHz, $CDCl_3$) δ 65.6 was absent; IR (film) 2197 cm^{-1} (C–D) was present.

(β-D)-**11a**: 4.93 g, 34 mmol, 98% yield. Spectral data were similar to those obtained for **11a** with the following exceptions: ^1H NMR (300 MHz, $CDCl_3$) δ 1.16-1.42 (m, 9 H); ^{13}C NMR (75 MHz, $CDCl_3$) δ 40.2 was absent; IR (film) 2130 cm^{-1} (C–D) was present.

(α-D,β-D)-**11a**: 5.25 g, 33 mmol, 94% yield. Spectral data were similar to those obtained for **11a** with the following exceptions: ^1H NMR (300 MHz, $CDCl_3$) δ 1.16–1.43 (m, 8 H), δ 3.49 was absent; ^{13}C NMR (75 MHz, $CDCl_3$) δ 40.2 and 65.6 were absent; IR (film) 2197 and 2097 cm^{-1} were present.

General Procedure for the Bromination of Alcohols to 12. PPh_3 (3.15 g, 12.0 mmol) and alcohol **11** (1.15 g, 10.0 mmol) were combined in CH_2Cl_2 (20 mL) and cooled to 0 °C. NBS (2.14 g, 12.0 mmol) was added over 2 h by means of a solid addition funnel, and the solution was stirred for 1 h at 0 °C and an additional 3 h at ambient temperature. The reaction mixture was concentrated to a slurry, and the resulting solids were dissolved in a minimum of CH_2Cl_2. To this solution was added 50 mL of petroleum ether at ambient temperature, and the mixture was then cooled to 0 °C. The supernatant was filtered *via* cannula, with a piece of filter paper attached to the end of the cannula, using a positive pressure of argon. The solids were washed sequentially with petroleum ether (2 × 25 mL) at 0 °C as before. This filtration sequence was performed two additional times. The organic fractions were combined and concentrated to approximately 15 mL and then filtered through a plug of basic alumina. Further concentration produced a residue, which was purified via Kugelrohr distillation (oven temperature 65–75 °C, <1 Torr) to give the corresponding bromide **12**.

12a: 3.97 g, 18 mmol, 94% yield; ^1H NMR (300 MHz, $CDCl_3$) δ 0.89 (t, J = 6.3 Hz, 3 H), 1.21–1.46 (m, 8 H), 1.61 (m, 1 H), 1.97–2.10 (m, 2 H), 3.43 (d, J = 2.8 Hz, 2 H), 4.93 (ddt, J = 10.2, 2.0, 1.1 Hz, 1 H), 4.98 (dq, J = 17.0, 2.0 Hz, 1 H), 5.78 (ddt, J = 17.0, 10.0, 6.7 Hz, 1 H); ^{13}C NMR (75 MHz, $CDCl_3$) δ 14.2, 19.7, 25.8, 32.0, 33.8, 34.8, 39.1, 39.4, 114.5, 138.6; IR (film) 3079, 2959, 2930, 2860, 1642, 1458, 1441, 992, 912 cm^{-1}; HRMS calcd for $C_{10}H_{19}Br$ m/z 218.0670, obsd m/z 218.0708.

(α-D)-**12a**: 3.58 g, 16 mmol, 88% yield. Spectral data were similar to those obtained for **12a** with the following exceptions: ^1H NMR (300 MHz, $CDCl_3$) δ 3.43 was absent; ^{13}C NMR (75 MHz, $CDCl_3$) δ 39.4 was absent; IR (film) 2250, 2190 cm^{-1} were present; HRMS calcd for $C_{10}H_{17}D_2Br$ m/z 220.0796, obsd m/z 220.0852.

(β-D)-**12a**: 4.60 g, 22 mmol, 65% yield. Spectral data were similar to those obtained for **12a** with the following exceptions: ^1H NMR (300 MHz, $CDCl_3$) δ 1.61 was absent; ^{13}C NMR (75 MHz, $CDCl_3$) δ 39.1 was absent; IR (film) 2097 cm^{-1} (C–D) was present; HRMS calcd for $C_{10}H_{18}DBr$ m/z 219.0733, obsd m/z 219.0724.

(α-D,β-D)-**12a**: 4.54 g, 20 mmol, 81% yield. Spectral data were similar to those obtained for **12a** with the following exceptions: ^1H NMR (300 MHz, $CDCl_3$) δ 1.61 and 3.43 were absent; ^{13}C NMR (75 MHz, $CDCl_3$) δ 39.1 and 39.4 were absent; IR (film) 2197, 2097, and 1995 cm^{-1} (C–D) were present; HRMS calcd for $C_{10}H_{16}D_3Br$ m/z 221.0859, obsd m/z 221.0830.

Preparation of Methylaluminoxane (MAO). Using standard Schlenk techniques, $Al(SO_4)_2 \cdot 14H_2O$ (18.6 g, 28 mmol) was taken up in toluene (125 mL) and cooled to 0 °C.[42] $AlMe_3$ (25 mL, Aldrich) was carefully transferred into the reaction vessel *via* cannula, the ice bath was removed, and the reaction mixture was stirred at room temperature under argon for 24 h. At this time, the solution was filtered through a Schlenk frit, and the solvent was removed *in vacuo* to give a glass-like solid. In an inert atmosphere box, the solids were scraped free from the sides of the flask and powdered. The solids were placed under vacuum for an additional 3 to 6 h, and the resulting MAO (5.05 g, 33% yield) was stored at –40 °C in the drybox. A fresh 0.5 M solution was made for each series of cyclizations by taking 0.349 g of MAO from the drybox in a stoppered Schlenk flask and diluting with toluene (12 mL). *Note*: The MAO solution was stored in the freezer at –20 °C between cyclization runs and was used within 48 h.

General Procedure for MgX_2-Promoted Cyclizations. A mixture of the appropriately labeled bromides **12a** and **12b** (1 mmol each) was added *via* gas-tight syringe over a 2 h period to activated Mg turnings (8.2 mmol, 0.20 g) suspended in Et_2O (2 mL) at room temperature. Analysis of the protonolysis products generated from an aliquot of the solution showed that 2–4% cyclization had occurred during formation of the Grignard reagent. The solution containing the Grignard mixture was stirred for an additional 1–2 h at room temperature and then was transferred *via* cannula to a –45 °C suspension of Cp_2TiCl_2 (2.4 mmol, 0.60 g) in CH_2Cl_2 (4 mL). The mixture was stirred at this temperature for 1 h, dodecane was added as an internal standard, and the mixture was warmed to room temperature. The reaction was monitored by capillary gas chromatographic analysis of samples obtained by cannula transfer of a small amount of the crude reaction mixture into approximately 0.3 mL of a 1 M solution of HCl in Et_2O at –78 °C. This sample was then filtered through a small column of basic alumina prior to injection onto the GC.

General Procedure for MAO-Promoted Cyclizations. Activated Mg (1.0 g, 41.0 mmol) was placed in a Schlenk flask with a stir bar and flamed dried under vacuum for 10–15 min. The flask was then allowed to cool under argon with vigorous stirring, at which time the Mg was suspended in 10 mL of THF and warmed to 45 °C. A mixture of the appropriately labeled bromides **12a** and **12b** (5 mmol each) was added dropwise *via* syringe to the Mg over a 2 h period. After addition was complete, the reaction was allowed to stir at 45 °C for 3 h and then cooled to ambient temperature. The Grignard solution was transferred *via* cannula to a –45 °C solution of Cp_2TiCl_2 (2.99 g, 12 mmol) in CH_2Cl_2 (35 mL), the Mg was washed with 5 mL THF, and the washings were transferred to the reaction mixture. After the transmetalation was stirred at room temperature for 1 h, the mixture was stored in the –20 °C freezer overnight. The solution was warmed to room temperature, pumped down to a burgundy oil, and then taken up in hexane (30 mL). Filtration of the hexane suspension was performed through a Schlenk frit, the solids were washed with hexane (2 × 15 mL) and toluene (2 × 5 mL), and the resulting solution was concentrated to an oil. The purified organometallic species was taken up in toluene (25 mL, to approximately 0.4 M), and dodecane was added as an internal standard. The stock solution was stored in the freezer (–20 °C) until used.

The organometallic solution was warmed to room temperature, and analysis of the protonolysis products showed that 3 to 9% cyclization had occurred prior to the addition of MAO. Aliquots of the organometallic solution (2.0 mL) were placed in evacuated and argon-purged flasks and cooled to –78 °C. The MAO (0.70–0.72 mL, 0.5 M in toluene) was added down the side of the flask slowly, and the mixture then was brought immediately to –45 °C and stirred for the indicated amount of time (5–20 min). The reaction was quenched by cooling the mixture to –78 °C and slowly adding anhydrous HCl in Et_2O, stirring for 5 min, and warming to room temperature. The quenched solution was passed down a pipette column of basic alumina prior to analysis by gas chromatography. Cis/trans assignments were made by comparison to an authentic sample prepared independently.

Acknowledgment. We are grateful to the National Institutes of Health (GM44163) for support of this research. Dr. Jon R. Young is acknowledged for preliminary investigations of related substrates, which prompted the authors to select the use of **14a** and **14b** for these competition studies. The authors would like to thank Professors Robert H. Grubbs (Caltech) and John E. Bercaw (Caltech) for enlightening discussions. N.S.B. wishes to thank the Organic Division of the American Chemical Society and Pfizer, Inc., for a Division of Organic Chemistry Graduate Fellowship and the General Electric Co. for an Academic Incentive Fellowship. Mass spectral data were obtained at the Michigan State University Mass Spectrometry facility which is supported, in part, by a grant (BRR-00480) from the biotechnology research technology program, National Center for Research Resources, National Institutes of Health.

Supplementary Material Available: Copies of ^1H NMR spectra of all compounds in the Experimental Section (13 pages) and tabulated relative rates used to calculate values in Table 1. This material is contained in many libraries on microfiche, immediately follows this article in the microfilm version of the Journal, and can be ordered from the ACS; see any current masthead page for ordering information.